THE UNIVERSITY OF WARWICK

Original citation:
Newby, Gemma E., Watkins, Erik B., Merino, Daniel Hermida, Staniec, Paul A. and Bikondoa, Oier. (2015) In situ Rheo-GISANS of triblock copolymers : gelation and shear effects on quasi-crystalline structures at interfaces. RSC Advances , 5 (126). pp. 104164-104171.

Permanent WRAP url:
http://wrap.warwick.ac.uk/75509

Publisher statement:
First published by Royal Society of Chemistry 2015
http://dx.doi.org/10.1039/C5RA20215A

For more information, please contact the WRAP Team at: publications@warwick.ac.uk

warwickpublicationswrap

highlight your research

http://wrap.warwick.ac.uk/

RSC Advances

PAPER

In situ *Rheo-GISANS* of Triblock Copolymers: Gelation and Shear Effects on Quasi-crystalline Structures at Interfaces

Gemma E. Newby,[*a] **Erik B. Watkins,**[b,c] **Daniel Hermida Merino** [d,e], **Paul A. Staniec**[f] **and Oier Bikondoa**[*g,h]

The behaviour of polymeric systems at surfaces and under flow is extremely important in many applications, ranging from drug delivery to lubrication. We have studied a model triblock copolymer in deuterated water combining in-situ rheology and grazing incidence small angle neutron scattering.
10 Several thermotropic phases appear as a function of the temperature, including a bicontinuous phase not present in the bulk. Moreover, gelation can occur following a different route depending on the concentration. We show that shearing can be used to monitor the structural integrity of the micellar systems and in some cases as a tool for modifying the thermotropic phases: an fcc (face centred cubic) phase is sheared into a hcp (hexagonally close packed) phase, and is then recovered by cycling the
15 temperature.

Introduction

Poloxamers or Pluronics® (trademark of BASF) are highly desirable nonionic amphiphilic triblock copolymers with block
20 structure PEO-PPO-PEO (PEO: polyethylene oxide; PPO: polypropylene oxide). They have been extensively studied in the bulk and are of considerable interest due to their chemical properties, colloidal behaviour and especially their extremely low toxicity[1]. The applications of Pluronics range from drug
25 delivery[2-4] to personal care products[5,6]. Pluronics in the bulk self assemble into ordered structures driven by the hydrophobic effect and influenced by changes in curvature[7,8,9]. PEO and PPO are both soluble in water at low temperatures (<15℃) but PPO becomes more hydrophobic as temperature is increased while
30 PEO remains essentially hydrophilic. However, the solubility of PEO decreases with temperature and induces a change in the optimum head-group area and a shrinkage of the corona[10,11]. Dehydration of the PPO core also occurs during a temperature increase, therefore having a higher density of the PPO core,
35 which has been shown using FTIR[12,13]; the trends of which are similar in both H_2O and D_2O[12]. Due to the shielding of hydrophobic PPO from the solvent, the PEO-PPO-PEO polymer chains assemble into structures ranging from spherical micelles to complex lyotropic and thermotropic liquid crystal phases[10]. The
40 different phases formed can be explained by changes in packing parameters of the micelles which in turn influence their shape and curvature (see figure 1)[9]. The packing parameter is defined as the ratio between the volume of the hydrophobic group and the area of the hydrophilic group multiplied by the length of the
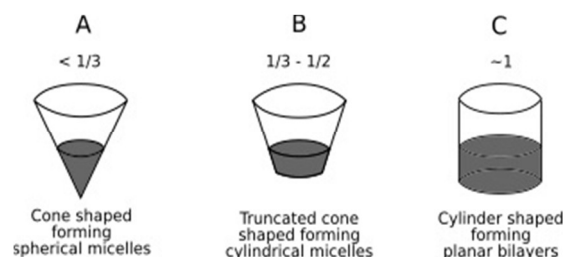45 hydrophobic group[9, 14].

Fig.1 Curvature diagrams and associated packing parameter, (adapted from reference 9), for block co-polymers which in turn form cubic (A), hexagonal (B) and lamellar (C) phases. The grey sections represent the
50 hydrophobic PPO groups (core) and the clear the hydrophilic PEO groups (corona)

Most applications and uses of Pluronics involve a confined environment in which surface or interfacial properties play a crucial role and may affect the stability and behaviour of the
55 different structural phases. For example, in the proximity of interfaces the solvent hydrodynamics control the motion and relaxation time scales of polymer solutions[15]. Although the behaviour of Pluronics at interfaces is extremely important to complete the understanding of the correlation between their
60 macroproperties and microstructure, especially for industrial and medicinal processes, the number of studies on Pluronics at surfaces or at interfaces is scarce. Here, we focus on the gelation and visco-elastic properties of Pluronic P85 at a silicon interface. P85 is a block amphiphile that has been tested as a carrier for
65 drug transport in the body[16]. We have studied the mesophase changes of P85 that occur as a result of the self-assembly of

micelles at the solid/liquid interface under external forces by combined grazing incidence small angle neutron scattering and in-situ rheology experiments at different temperatures and two different concentrations to relate mechanical response to structural changes.

Experimental

Materials

Pluronic P85 was kindly donated by BASF® and was used as received. P85 has an average molecular weight of 4600 g mol^{-1} and is denoted $E_{26}P_{41}E_{26}$.

Sample Preparation

The solutions at two distinct concentrations, (30 and 40 wt%), were prepared by dissolving the Pluronic into D_2O at 4 °C using an ice bath and magnetic stirrer. D_2O was used to reduce background scattering and maximize the contrast with the copolymers. Once the solutions had fully dissolved they were stored in the fridge overnight to ensure complete dissolution and stability. At 4 °C both of the solutions are in liquid phases.

Rheo – GISANS

The experiments were carried out on FIGARO at the ILL, Grenoble, France[17]. FIGARO is a time of flight (TOF) neutron reflectometer with GISANS capabilities. Measurements were performed using wavelengths from 1.5 to 20 Å with a 7.0 % $\Delta\lambda/\lambda$ wavelength resolution. An angle of 0.4° between the incident beam and the sample plane was employed yielding a critical wavelength of 6.0 Å for the silicon/D_2O interface. Neutrons were detected using a two dimensional ^{3}He detector. An Anton Paar 501 rheometer, employing a cone and plate geometry, was used on the FIGARO sample table for the experiments. The 5 cm diameter cone has a 49 μm truncated base and angle of 1°. A 7x7 cm^2 by 1 cm (thickness) silicon crystal was used as a plate. This silicon crystal was fixed on the rheometer so that the neutron beam travels up through the crystal, probes the solid / liquid (sample) surface and is then scattered back through the crystal (see Fig. 2). The beam footprint on the crystal was, on average, 1 cm (width) by 4 cm (length).

The cold solutions were pipetted onto the silicon crystal, which was at the same temperature of the solutions, then the cone lowered into position carefully allowing for any spillage of the sample to be trimmed, followed by an equilibration period. From previous experiments[11,18] the 30 wt% samples are known to gel between 20 and 25 °C so the temperature was initially ramped up to 20 °C and held on for an hour. Subsequently the temperature was increased again by 2 °C and scattering images collected. For the 40 wt% sample the temperature was initially set at 10 °C allowing easy compression in the liquid phase. The temperature of the system was then gradually increased since gelation occurs between 10.5 and 13 °C[11]. A 1 °C /min heating rate was used. Subsequent structures for both concentrations were monitored via GISANS over specified temperature ranges. At selected temperatures a logarithmically increasing shearing protocol[19] was adopted to investigate the influence of external forcing on the structures formed.
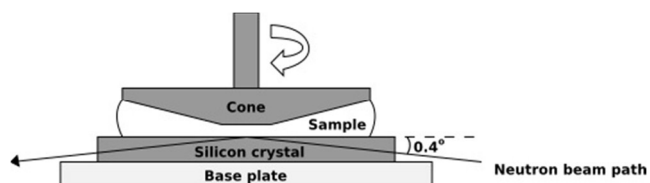

Fig.2 Sample environment for Rheo – GISANS. The standard 50 mm (diameter) cone is used on the adapted base plate. The cone has a truncation of 49 μm and a 1° angle, therefore the gap at the edge is 436 μm and the loading volume is 0.6 ml. Silver paint was used to glue the crystal onto the mounting plate.

The exposure time for a GISANS image was one hour. The images were taken under two types of shear which can help characterise dynamic mechanical responses[19]: oscillatory shear for viscoelastic behaviour and rotational shear for viscous behaviour. The protocols adopted for the oscillatory experiments were an angular frequency of 5 rad / s and strain of 0.1 %, both of which are within the linear viscoelastic region of the samples[6]. The GISANS images were taken under the controlled strain of the rheometer and at constant temperatures. For the rotational experiments, shear rates of 0.01, 0.1, 1, 10 and 100 s^{-1} were used in the controlled shear rate mode. The shear rate was increased to a required value then held whilst a GISANS image was recorded. GISANS data was collected as a function of TOF and the out-of-plane (2θ) and in-plane scattering angles (α_f). Reduction of the raw data to Q_y vs Q_z (in-plane vs out-of-plane) space was completed using in-house software. To extract the GISANS intensity, a wavelength (λ) range of 7.5-9.5 Å was chosen to discriminate neutrons that impinged on the sample below the critical momentum transfer. These intensities were normalized by the incident neutron wavelength spectrum and corrections were applied to account for gravitational effects on the neutron trajectories. Using the equations $Q_y = 2\pi/\lambda \ \sin(2\theta) \ \cos(\alpha_f)$ and $Q_y = 2\pi/\lambda \ \sin(\alpha_i) + \sin(\alpha_f)$, the measured angle and TOF data was transformed to momentum transfer space. Based on the detector pixel width and the size of the TOF bins, matching ranges in Q space were calculated and the intensity was distributed uniformly over the corresponding pixels. This transformation yielded a regularly gridded array of intensity conserving the total number of detected neutrons.

The Q_y vs Q_z (Å^{-1}) intensity maps obtained from the data reduction procedure were analyzed by indexing the peak positions and completing line integrations in both the horizontal and vertical directions over selected ranges of momentum transfer values. These line profiles enable more quantitative analysis of the images in the way of correlation separation and relative degree of order within the system.

The rheological data was extracted and analyzed using the Rheoplus software from Anton-Paar GmbH[20]. The oscillatory results are presented as time sweeps to monitor the viscoelastic properties of the system throughout the GISANS exposure time. The viscosity curves used here were extracted from the rotational time sweeps at various shear rates and the error bars calculated from the standard deviation once the sample had reached a suitable degree of stability. Lines as guides for the eye were then overlaid to aid in the explanation of the flow behaviour of the systems.

Table 1 Temperature induced gel phases

System concentration (wt%)	Phase	Temperature reached (°C)	Figure	Comments
30	Soft micellar gel	22	4 A	Starting temperature of the experiment
	FCC	24.9	4 B	FCC phase disappearing at 50.5 °C
	Lamellar	52.0	-	
40	Soft micellar gel	11.2	5 A1	Starting temperature of the experiment
	Lamellar	12.0	5 A2	Seen in a very narrow range
	Cubic BCC	12.4	5 B	Start of signs for the BCC phase
	BCC	30.0	6 A	More defined BCC
	Bi-continuous	31.5	6 B	Lamellar phase reached during shearing protocol

Results

Two selected concentrations of Pluronic P85 were probed, 30 wt% & 40 wt%. These two concentrations cover most of the possible phases of P85[5]. The 30 wt% system was used to gain enhanced insight into the FCC structure upon gelation and formation of lamellar phases. The 40 wt% system was used to track the gelation into a HCP phase followed by cubic and bi-continuous phases. The results about the gelation mechanism for each sample are introduced first, followed by the behaviour of each sample upon shearing. Table 1 and figure 3 summarise the main thermotropic phases that have been obtained in this study.

Gelation and temperature induced phases

In order for gelation to occur the P85 system must be at a high enough concentration for the spherical micelles to interact, which is substantially greater than the critical micelle concentration (e.g. 0.03 wt% at 37 °C) of the system[21].
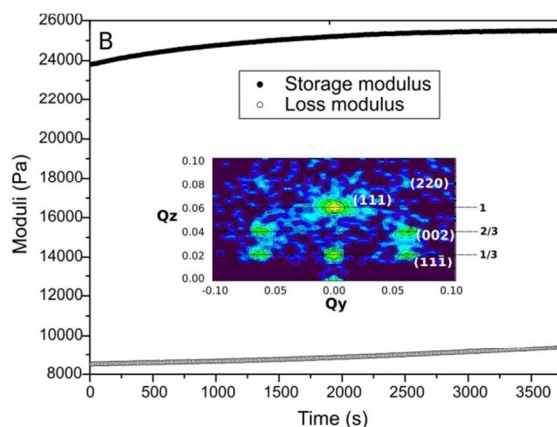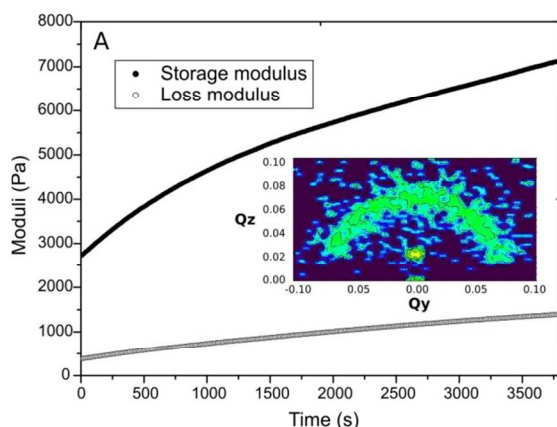
Fig. 3 Cartoon representations of the main phases observed during the study. A spherical micelle has also been included representing the initial form after micellization. In the BCC and FCC images the PPO core is not shown.

P85 spherical micelles have core radii between 3 and 6 nm depending on concentration and temperature[5, 22 – 25]. When the gelation transition occurs, the mechanical properties of the system change. The elastic and viscous responses of the system to strain are described by the storage modulus and the loss modulus, respectively[26]. We have studied the viscoelastic response by oscillatory shear measurements. Upon gelation influenced by temperature, concentration, or both, the system self-organizes into quasi-crystalline structures. Micelles follow the spherical (cone) to cylindrical (truncated cone) to planar (cylinder) transformations and corresponding morphologies which results mainly from hydrophobicity and consequent dehydration of the micelles[27,13].

Gelation of 30 wt% P85

We started our measurements at 22 °C in a soft gel phase consisting of correlated micelles and a gradual increase of the storage modulus to 8 kPa. The FCC phase was reached at 24.9 °C (see Fig. 4, B) with a storage modulus of 25 kPa; in the range of a typical hard gel[28].

Fig. 4 GISANS images of the 30 wt% sample under oscillatory motion (0.1 % strain and 5 rad/s) at 22.6 °C (A) and 24.9 °C (B), along with their corresponding rheological profiles. The system undergoes a gelation pathway towards a hard cubic gel (FCC phase indicated by the indexed peaks).
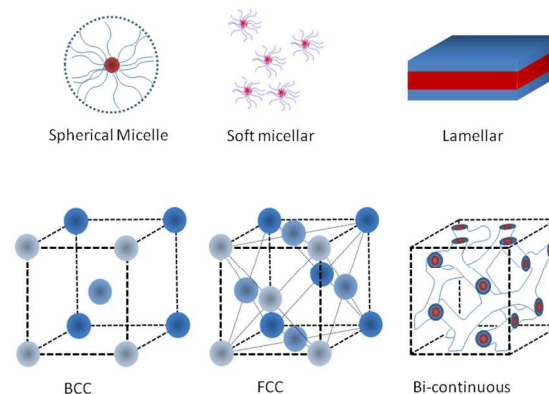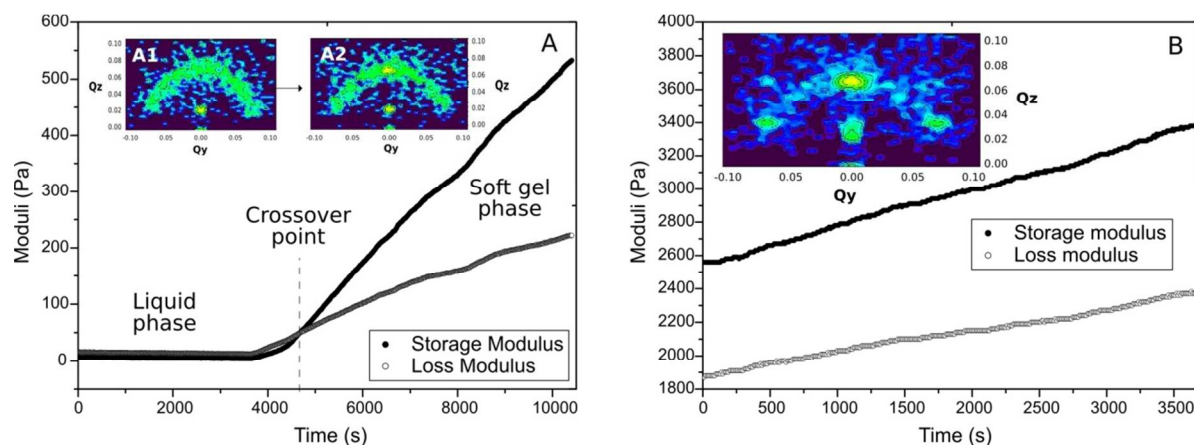
Fig. 5 GISANS images and rheological profiles of the 40 wt% sample under oscillatory motion (0.1 % strain and 5 rad/s).   A – 10 °C (A1) and 11.2 °C (A2) inset into the profile showing the initial phase change into a soft gel. The gel point is defined as the point at which the storage and loss moduli cross, i.e. the crossover point (indicated by the dotted line on the graph). B- Further gelation of the 40 wt% system through a hexagonal phase with two very faint extra reflections at 12.4 °C, indicating the formation of a body centered cubic phase

In the bulk, the 30 wt% sample gels between 20 and 25 °C[10]. Thus, the gelation of 30 wt% P85 observed in this study is consistent with previous measurements performed in the bulk, the only difference being that it occurred at a lower temperature. The difference in gelation temperature may be due to confinement at a surface, which affects the curvature of the micelles, perturbing the transition temperature. The FCC structure has an interlayer distance of $a = 18 \pm 0.5$ nm, determined from the (111) Bragg peak position[29]. This FCC phase then changes into a lamellar phase at 52 °C (not shown).

Gelation of 40 wt% P85

The measurements were started at 10 °C where the storage and loss modulus are very small and the system behaves like a viscous liquid. A correlated micellar phase was observed (Fig. 5, A1). The correlation distance in the liquid phase was determined from the Q position of the ring to be 92 ± 3 Å. As the temperature was slowly increased to 11.2 °C to encourage gelation (see Fig. 5, A2), the correlation peak became better defined indicating enhanced order, before processing through a very short lived lamellar phase into HCP / cubic. Both the PEO and PPO are less hydrophilic at this low temperature which explains the presence

of the short lived lamellar phase. The system formed a hard gel at 12.4 °C; this is shown by the moduli in the rheology and the peaks in the scattering image, shown in figure 5 B. Unlike in the bulk[10] the expected FCC phase is not initially formed; the HCP seems to be more prominent with two faint extra reflections; we hypothesize that this may be due to the influence of the interfacial energy.

After the initial gelation of the 40 wt% system into the HCP phase, there is some evidence of the BCC phase at 30 °C indicated by the 200 reflection (Fig. 6, A) with an interlayer distance of $a = 14 \pm 0.4$ nm (from the (110) reflection). When the temperature of micellar systems is increased, dehydration of the coronas initially occur, followed by shrinkage of the micelles and rearrangement into more energetically favourable conformations. As the temperature increases, dehydration and shrinkage modifies the curvature of the micelles resulting in the phase changes observed. The micelles gradually evolve from a truncated cone into a cylinder. A bicontinuous phase not previously observed in bulk materials is formed at 31.5 °C, (see Fig. 6, B), which is consistent with branched cylindrical micellar aggregates, where the packing parameter of the micelles is between 1/2 and 1.

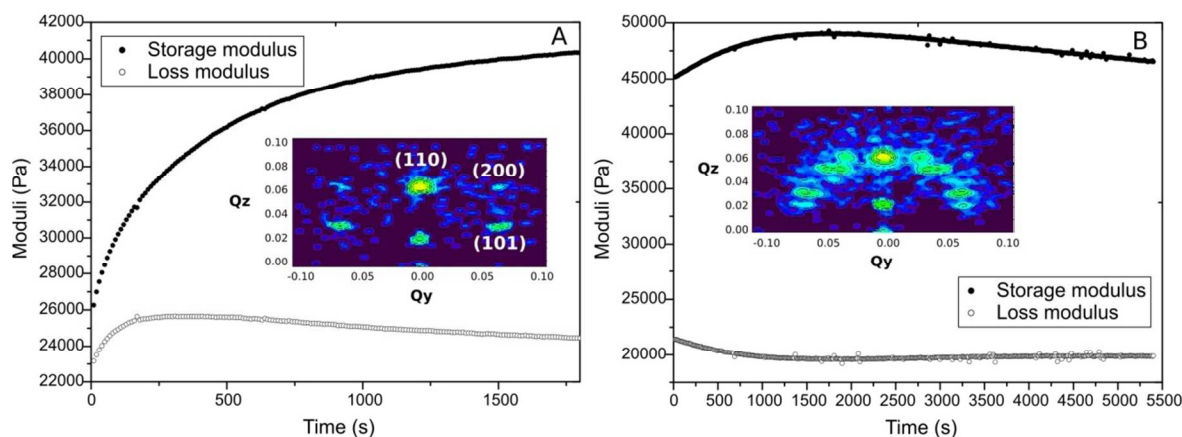**Fig. 6** Oscillatory rheological profiles and corresponding GISANS images of the 40 wt% system. A – The structure and properties when increasing from 28 °C gradually to 30 °C in which the faint BCC reflections can still be seen. B – The bi-continuous phase is reached (31.5 °C). The storage modulus is greater than that of the FCC structures seen before as a result of the branching of the cylindrical micelles.

Shearing

Cubic, hexagonal and lamellar phases are very prominent in many block copolymers, such as Pluronics and are used in drug delivery[30], membranes[31], cancer therapy[32] and industrial applications, emulsifiers and lubricators[33]. For such applications, knowing the behaviour under shear is vital. Here we investigate the mechanical response of cubic, bi-continuous, hexagonal and lamellar phases.

Structures were sheared until they began to melt. For the 30 wt% system, in the lamellar phase, the shear test was stopped at 10 s^{-1} since the viscosity of the system already plummeted to 1 Pa.s at this point. The protocol was started at 0.1 s^{-1} due to a plateau region at very low shear rates; a certain rate was required before the system was initially disturbed. The 40 wt% system in the bicontinuous phase was also only sheared up to a shear rate of 10 s^{-1} since at this point a lamellar phase was reached.

Shearing of 30 wt% P85

We performed rotational shear rheometry measurements on two selected phases: FCC phase at 25 °C and lamellar phase at 54 °C.

Effect of shear on the FCC phase at 25 °C (30 wt%)
The results of the shear response are presented in figure 7. There is a breakdown of the FCC phase beginning almost immediately at a shear rate of 0.01 s^{-1} followed by transitions through FCC/HCP mixed phases into a hexagonal structure. These changes occur because of the induced curvature changes of the micelles themselves, as a result of external forces. To form spherical micelles a cone shape is adopted with a packing parameter less than 1/3. Under shear, the micelles elongate into elliptical / cylindrical structures as a result of their packing parameter changing to be between 1/3 and 1/2. This occurs because the hydrophilic groups initially feel the shear and compensate by decreasing their effective area which in turn increases the packing parameter. The sample was allowed to relax after the shear experiment but even after three hours the FCC structure did not recover although most of the mechanical behaviour did, (see Fig. 7, F), which suggests that shearing may have locked the sample in a metastable state. In order to completely recover the initial structure the shearing history must be completely removed. Rejuvenation was achieved by cooling the sample down slightly to reach the disordered phase, followed by heating it back up. Once the original FCC phase was recovered the structure and properties were tracked upon further temperature increases.
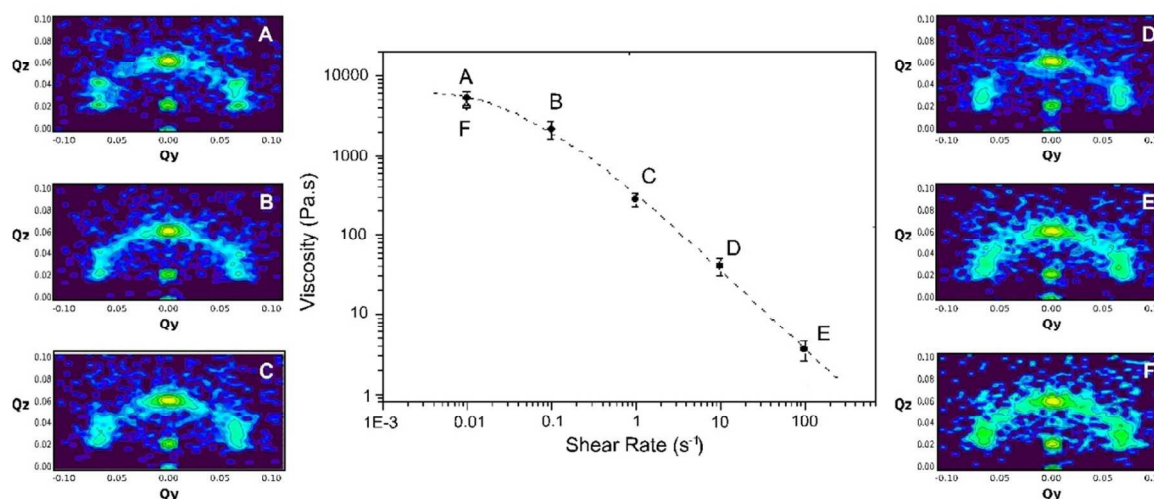
Fig. 7 Shearing and viscosity curve at 25 °C for the 30 wt% system. Each point on the viscosity curve was collected for one hour. There is a small zero viscosity region with a plateau value of approximately 6 kPa.s followed by the shear thinning region. The recovery of the sample (open symbol at 0.01 s^{-1}) shows that from a rheological perspective the sample has relaxed back to its original state at the low shearing rate but has not recovered from the structural perspective (image F)

RSC Advances Accepted Manuscript
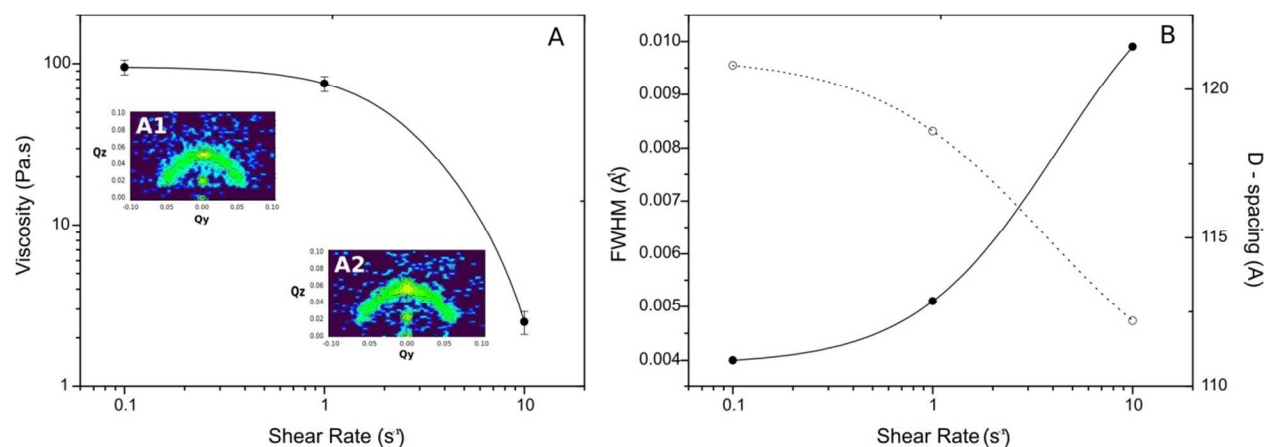
Fig.8 A – Shearing curve of the lamellar phase formed by the 30 wt% sample at 54 °C up to a shear rate of 10 s^{-1} (at higher rates the sample melts). The viscosity of the system is fairly low at the lowest shear rate indicating the lamellar sheets starting to flow over one another. As the shear rate is increased the viscosity begins to drastically decrease signifying disorder of the lamellae within the system. B – Relative broadness of the lamellar peak and spacing as a function of shear rate for the 40 wt% system. The solid symbols represent the FWHM of the main lamellar peak and the hollow symbols represent the resultant D-spacing. It can be seen that the lamellae become closer together and lose long range order with increasing shear.

Effect of shear on the lamellar phase at 54 °C (30 wt%)

The results of shearing are presented in figure 8. The viscosity is much lower than that at 25 °C which suggests that the cubic phase is no longer present; the lamellar sheets flow easier reducing the viscosity of the system by a factor of 10, (under selected shear rates), as can be seen when comparing the storage moduli in figures 7 and 8. This is expected since sheets flow with less hindrance producing lamellar flow. In order to analyze the viscosity changes further linear cuts along $Q_y = 0$ Å^{-1} of the GISANS images were taken and Gaussian peaks fitted to the lamellar first order. The full width half maximum and the centre of the peaks were then extracted from these fits and hence the order and d-spacing's of the lamellar sheets determined respectively as a function of shear rate, the results of which are presented in figure 8, B. It can be seen that both the FWHM and d-spacing significantly change between a shear rate of 1 and 10 s^{-1}. This effect can be explained by the lamellar sheets becoming more disordered (indicated by a broader peak) as a result of the higher shear rates. This suggests that the increased shear starts to introduce turbulence into the system which in turn causes the lamellar structure to break slightly and tumble.

Shearing of 40 wt% P85

For the 40 wt% sample, we tested the effect of shearing on the BCC phase at 12.4 °C and on the bi-continuous phase at 31.5 °C.

Shearing at 12.4 °C (BCC phase, 40 wt%)

The phase present at 12.4 °C was sheared from 0.01 to 100 s^{-1}, then slowed back down to 0.01 s^{-1} and finally left for 2 hours to relax. This protocol was adopted to try to order the BCC structure to highlight the extra reflections and attempt to partially melt it before letting it recover. Selected results can be seen in figure 9. The optimum shear rate for aligning the BCC phase is 0.01 s^{-1} since above this value, the extra reflections faded and the peaks began to merge into a ring indicating tumbling. When the shear was returned to 0.01 s^{-1} the rheological properties recovered as indicated in figure 9 on the viscosity curve. Both the structure and properties of the system recovered after 2 hours. At this stage, the temperature of the system was increased again to see if

further phases could be reached.

Shearing the bi-continuous phase at 31.5 °C (40 wt%)

The bi-continuous phase evolves rapidly with shear into a lamellar phase, as shown in figure 10. The bi-continuous structure completely changes into the lamellar phase under a shear rate of 10 s^{-1} but this change is not fully reversible; after reducing the shear rate back to 0.01 s^{-1}, the viscosity of the system was reduced by half whilst remaining in the bicontinuous phase, which could be a result of the branched nature of the bi-continuous phase. The viscosity curves have a non-standard shape as a result of this branched bi-continuous structure and have an initial higher viscosity than the other phases. The initial low shearing rate aligns some of the branches in the bi-continuous structure causing initial decrease in viscosity. After this, a certain shear force is required to disrupt the branching and this induces the melting into the lamellar structure.

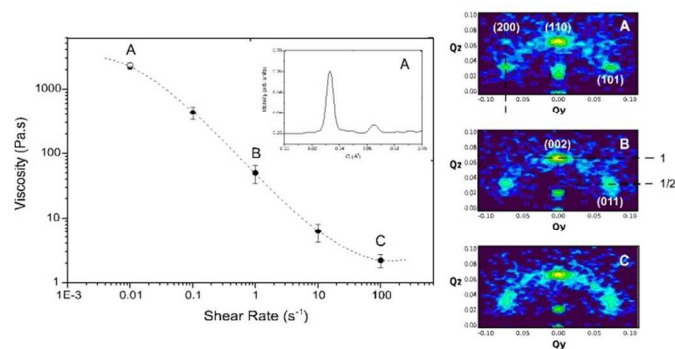**Fig.9** Viscosity curve and related GISANS images of the 40 wt% system at 12.4 °C. Each point on the viscosity curve was collected for one hour. Three standard regions are present in the viscosity curve; zero shear viscosity, shear thinning and infinite shear viscosity. The GISANS images on the right, from top to bottom, are shearing at 0.01, 0.1 and 1 s^{-1}, respectively. The hollow point on the viscosity curve at a shear rate of 0.01 s^{-1} is during relaxation after the shearing protocol. The inset shows vertical line integration from image A in which a BCC structure is observed. The ratio of the peak intensities is 6:1
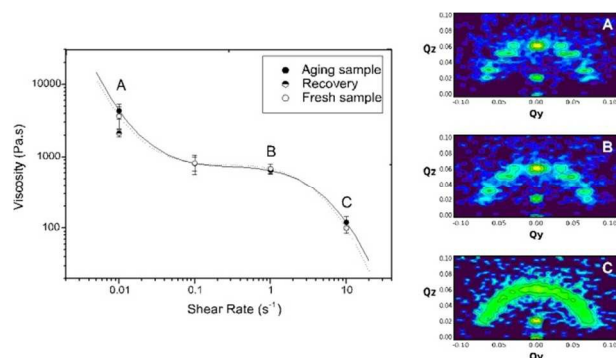
Fig.10 Rheological profile and selected GISANS images of the 40 wt%
sample under rotational motion at 31.5 °C. It can clearly be seen from
this graph that the sample did not recover completely due to the
branching nature of the phase; the viscosity of the system only
recovered to 2.5 kPa whereas it started at nearly 5 kPa.

Since the system had a shearing history through other phases the
experiment was repeated with a fresh sample. The fresh 40 wt%
sample was loaded into the rheometer at 10 °C (the same as the
first sample) and directly heated to the temperature at which the
bi-continuous structure presented itself previously (31.5 °C).
The BCC phase was observed again, beginning at 12.4°C (not
shown). Once the bi-continuous phase was reached, the sample
was sheared as previously. The results with this sample with no
shearing history (figure 10 crosses and dashed line) coincide with
the values found previously, indicating that the shearing history
from the initial experiment had very little effect on the viscosity
curve. This suggests that the resting time of 2 hours between
different shear conditions was enough for the structure to relax
into its equilibrium state.

Discussion

Gelation mechanisms are extremely important in the medical and
pharmaceutical sectors due to their main uses; in-vivo delivery of
pharmaceutical agents, where the agent is delivered as a cool
liquid and gels upon warming to body temperature as to not
damage proteins and in topical applications such as wound and
burn healing[34] where a barrier is formed over the troubled area. It
is crucial for such applications to know exactly which kind of
thermotropic phases may develop as a function of the
temperature. But in such applications, and in many other sectors,
including industrial (processing[35], paint, emulsifiers), personal
care (cream, shampoo), and medical (ionic conductivity
membranes, stabilizers[33]), it is also necessary to determine the
effects of shear on the system. Shearing may be needed for some
systems to reach their ideal viscosity for transfer or potential
applications. Our study is focused on the model system P85 at
two selected concentrations and shows the two typical gelation
routes that occur in Pluronic P85: gelation into a cubic phase and
through a hexagonal phase[22, 36]. To our knowledge the bi-
continuous phase formation in Pluronics is rare. In bi-continuous
phases, the interfacial area between the amphiphiles and the
solvent is reduced and interconnected domains of polymers
coexist. Bi-continuous networks have a strong potential
technological interest. For example, bi-continuous phases have
been used in hybrid bulk heterojunction solar cells[37] and can even
show exotic optical properties such as a negative index of

refraction[38]. The appearance of a bi-continuous phase in our
measurements, in contrast with bulk results[39], could be due a
metastable state that depends on sample history; temperature and
shear. Our result shows that methods exploiting the combination
of temperature and shear induced gelation mechanisms offer new
paths to produce tailored phases in view of potential applications.
Flow rate is an extremely important factor for the integrity of the
structures. We have observed that the structures recover, in most
of the cases, after 1 – 2 hours in the absence of shear even if they
are still compressed in the rheometer. The shearing history also
plays an important role. For the particular case of the bi-
continuous phase (40 wt% at 31.5 °C) we have observed that the
results obtained with a fresh sample and samples with a shear
history that has gone through lower temperature thermotropic
phases are alike. However, our rotational shear experiments show
that once the bi-continuous phase has been reached, further
shearing modifies the bi-continuous phase irreversibly: although
by reducing the shearing to the elastic regime the bi-continuous
phase is recovered, as GISANS results show, the viscoelastic
properties are modified. However, we note that GISANS yields
information about ensemble averaged properties but locally there
may be important differences caused by shearing between the two
systems and which may alter the mechanical properties. Local
probes or experiments that look into the polymer dynamics could
provide more information. Our work demonstrates the importance
of performing combined experiments to access complementary
information.

Conclusions

The gelation and phase behaviour of P85 at a compressed and
sheared interface is extremely rich, even more so than in the
bulk[11,18]. Importantly, it has been observed that shearing can be
used to both induce phase changes within micellar systems and to
monitor the durability and breakdown of the consequent phases.
This is an extremely important phenomenon as a result of the
structural integrity required in applications ranging from
templating[40] to drug delivery[2].

Notes and references

*Corresponding authors
[a] *ESRF- The European Synchrotron. CS40220. F-38043 Grenoble Cedex
9, France; E-mail: gemma.newby@esrf.fr*
[b] *MPA-11, Los Alamos National Laboratory, Los Alamos, New Mexico,
USA*
[c] *FIGARO, ILL- Institut Laue-Langevin, 71 avenue des Martyrs, 38000
Grenoble, France*
[d] *DUBBLE CRG BM26 ESRF, Netherlands Organization for Scientific
Research, ESRF-The European Synchrotron, 71, Avenue des Martyrs,
Grenoble, France, France*
[e] *Dutch Polymer Institute DPI, P.O. Box 902, Eindhoven 5600 AX, The
Netherlands*
[f] *Diamond Light Source Ltd., Diamond House, Harwell Science and
Innovation Campus, Didcot, Oxfordshire, OX11 0DE, UK*
[g] *XMaS, The UK CRG Beamline. ESRF- The European Synchrotron.
CS40220. F-38043 Grenoble Cedex 9,France; E-mail:
oier.bikondoa@esrf.fr*
[h] *Department of Physics-University of Warwick. Gibbet Hil Road.
Coventry CV4 7AL, UK*

1   K. Huang, B. Lee and P. B. Messersmith, *Polymer Preprints*, 2001, **42**, 147
2   WD. Ma, H. Xu, C. Wang, SF. Nie and WS. Pan, *International Journal of Pharmaceutics*, 2008, **350**, 247
3   AV. Kabanov and VY. Alakhov, *Critical Reviews in Therapeutic Drug Carrier Systems*, 2002, **19(1)**, 1
4   AV. Kabanov ,EV. Batrakova and VY. Alakhov, *Journal of Controlled Release*, 2002, **82(2)**, 189
5   P. Alexandridis and TA. Hatton, *Colloids and Surfaces A: Physicochemical and Engineering Aspects,* 1995, **96**, 1
6   D. Cohn, A. Sosnik and S. Garty, *Biomacromolecules*, 2005, **6**, 1168
7   L. Reidar, W. Lutz and D. Richter, *Advances in Polymer Science*, 2013, **259**, 51
8   RG. Larson, *The Structure and Rheology of Complex Fluids*, 1999, Oxford University Press, New York
9   IW. Hamley, *Introduction to Soft Matter*, 2007, John Wiley & Sons, Ltd.
10 K. Mortensen, *Journal of Physics: Condensed Matter,* 1996, **8**, A103
11 GE. Newby, IW. Hamley, SM. King, CM. Martin and NJ. Terrill, *Journal of Colloid and Interface Science*, 2009, **329**, 54
12 Y-L. Su, J. Wang and H-Z. Liu, *Journal of Physical Chemisty*, B 2002, **106**, 11823
13 C. Guo, H-Z. Liu and J-Y. Chen, *Colliod and Polymer Science*, 1999, **277(4)**, 376
14 JN. Israelachvili, DJ. Mitchell and BW. Ninham, *Journal of Chemical Society, Faraday Transactions 2*, 1976, **72**, 1525
15 TA. Witten and PA Pincus, *Structured Fluids: Polymers, Colloids, Surfactants*, 2010, Oxford University Press
16 EV. Batrakova and AV. Kabanov. *Journal of Controlled Release,* 2008, **130**, 98; and references therein.
17 RA. Campbell, HP. Wacklin, I. Sutton, R. Cubitt and G. Fragneto, *European Physics Journal Plus*, 2011, **126**, 107
18 K. Mortensen and JS. Pedersen, *Macromolecules*, 1993, **26**, 805
19 TG. Mezger, *The Rheology Handbook*, 2006, Vincentz Network GmbH & Co KG, Hannover
20 Rheoplus Software Manual Version 4, Anton-Paar GmbH.
21 IR. Schmolka and AJ. Raymond, *Journal of the American Oil Chemists Society*, 1965, **42**(12), 1088
22 K. Mortensen, *Europhysics Letters*, 1992, **19**(7), 599
23 K. Mortensen, *Jornal de Physique IV, Collaque C8, suppliment au Jornal de Physique I*, 1993, **3**, 157
24 JS. Pedersen and MC. Gerstenberg, *Colloids and Surfaces A: Physiochemical and Engineering Aspects*, 2003, **213**, 175
25 B. Hammouda, *European Polymer Journal*, 2010, **46**, 2275
26 RAL. Jones, *Soft Condensed Matter*, 2002, Oxford University Press; 1 edition
27 G.Wanka, H.Hoffmann and W. Ulbricht, *Macromolecules*, 1994, **27**, 4145
28 S. Hvidt, EB. Jørgensen, K. Schillevn and W. Brown, *Journal of Physical Chemistry,* 1994, **98**, 12320
29 D-M. Smilgies and DR. Blasini, *Journal of Applied Crystallography*, 2007, **40**, 716
30 A. Torcello-Gómez, M. Wulff-Pérez, M. J. Gálvez-Ruiz, A. Martín-Rodríguez, M. Cabrerizo-Vílchez and J. Maldonado-Valderrama, Advances in *Colloid* and *Interface Science,* 2014, **206**, 414
31 SS. Soni, KB. Fadadu and A Gibaud, *Langmuir*, 2012, **28**, 751
32 S.Miyazaki, S. Takeuchi, C. Yokouchi and M. Takada, *Chemical* and *Pharmaceutical Bulletin.*, 1984, **32(10)**, 4205
33 IR. Schmolka, *Journal of the American Oil Chemists Society*, 1977, **54**, 110
34 RM. Nalbandian, RL. Henry, KW. Balko, DV. Adams and NR Neuman, *Journal* of *Biomedical Materials Research,* 1987, **21**(9), 1135
35 *Properties and Behavior of Polymers*, 2011, Wiley-Blackwell; 1st Edition
36 F. Artzner, S. Geiger, A. Olivier, C. Allais, S. Finet and F. Agnely *Langmuir*, 2007, **23**, 5085
37 EJW. Crossland, M. Kamperman, M. Nedelcu, C. Ducati, U. Wiesner, DM. Smilgies, GES. Toombes, MA. Hillmyer, S. Ludwigs, OU. Steiner and HJ. Snaith, *Nano Letters*, 2009, **9**, 2807
38 K. Hur, Y. Francescato, V. Giannini, SA. Maier, RG. Hennig and U. Wiesner, *Angewandte Chemie,* 2011, **123**, 12191
39 IW. Hamley, *Current Opinion in Colloid & Interface Science*, 2000, **5(5-6)**, 341
40 DR. Dunphy, PH. Sheth, FL. Garcia and CJ. Brinker, *Chemistry of Materials*, 2015, **27(1)**, 75

In situ *Rheo-GISANS* of Triblock Copolymers: Gelation and Shear Effects on Quasi-crystalline Structures at Interfaces

Gemma E. Newby,*[a] Erik B. Watkins,[b,c] Daniel Hermida Merino [d,e], Paul A. Staniec[f] and Oier Bikondoa*[g,h]

Graphical Abstract

The behaviour of polymeric systems at surfaces and under flow is extremely important in many applications, ranging from drug delivery to lubrication. We have studied a model tri-block copolymer in deuterated water combining in-situ rheology and grazing incidence small angle neutron scattering. Several thermotropic phases appear as a function of the temperature, including a bicontinuous phase not present in the bulk. Moreover, gelation can occur following a different route depending on the concentration. We show that shearing can be used to monitor the structural integrity of the micellar systems and in some cases as a tool for modifying the thermotropic phases: an fcc (face centred cubic) phase is sheared into a hcp (hexagonally close packed) phase, and is then recovered by cycling the temperature.

RSC Advances Accepted Manuscript